Ultrasonic Measurements of Contact Stiffness Between Rough Surfaces

Grzegorz Starzynski

Institute of Fundamental Technological Research,
Polish Academy of Sciences,
Pawinskiego 5B, 02-106 Warsaw, Poland,
e-mail: gstarz@ippt.gov.pl

Ryszard Buczkowski

Division of Computer Methods,
Maritime University of Szczecin,
ul. Poboznego 11, 70-507 Szczecin, Poland,
e-mail: rbuczkowski@ps.pl

We have used an ultrasonic method to determine the normal and shear stiffness for three different surfaces. The degree of hysteresis for the loading/unloading and stiffness ratio is a function of roughness. Nonlinear contact stiffness characteristics are obtained. The ratio of tangential to normal stiffness K_T/K_N slowly increases in proportion to normal loading. The novelty of our setup is that at the same time we can measure the reflection coefficient, obtain results for three transducers simultaneously, and measure the approach as a function of load. The presented experimental results of normal contact stiffness measurements have been used for the verification of our theoretical model based on a fractal description of rough surfaces (Buczkowski et al., "Fractal Normal Contact Stiffness of Rough Surfaces," Arch. Mech. (submitted for publication). [DOI: 10.1115/1.4027132]

1 Introduction

The measurement and prediction of both normal and tangential stiffness has been studied by a number of authors [1–7]. Akarapu et al. [3] pointed out that the contact area and normal stiffness rise linearly with the applied load. Medina et al. [4] proposed a simple analytical model based on the classical work of Greenwood and Williamson and predict that tangential stiffness is proportional to normal load and independent of the asperity radius and Young's modulus. Pohrt and Popov [5,6] suggest a sublinear relationship between the normal stiffness and the nominal pressure. They state that the power-law relation observed for slowly applied forces is valid for all applied forces, with the exponent varying from 0.50 to 0.85, depending on the fractal dimension. The results presented by Pohrt and Popov [5,6] are not confirmed by Pastewka et al. [7], who have shown that the contact stiffness cannot be described by a power law for all applied forces and this would correspond to a straight line on a log-log scale only. Several authors note [2,5,8–11] that the expression for the micro-asperity contribution to the total elastic energy and elastic stiffness depends on the elastic coupling between asperities. Some of them state that any derivation neglecting this interaction cannot describe the correct physics of realistic rough surfaces. Barber [10] has identified an analogy between electrical conduction and contact stiffness, in which electrical conduction at any load is proportional to the elastic normal stiffness. This relation has been extended to the contact of finite bodies [11]. Measurements of the tangential contact stiffness between rough surfaces manufactured from titanium alloy using the digital image correlation method have recently been investigated by Kartal [12].

Various measuring setups have been used to use the changes in the ultrasound wave reflection coefficient for the assessment of the real contact area and contact stiffness [13–15]. In Refs. [16,17] the heads for 2.5 MHz longitudinal and transverse waves are used for examining the contact between two aluminum specimens; the setup arrangement, however, is allowed to apply only low loads (up to 4 MPa).

Another study [18] investigates the reflection coefficient for cyclic loads over the yield limit with a broadband transducer of 10 MHz longitudinal waves. An assessment of the interfacial stiffness ratio K_T/K_N for grit-blasted specimens is presented in Ref. [19].

2 Ultrasonic Setup

We have determined the experimental values of both the tangential and normal contact stiffness from ultrasonic measurements by predictions of the reflection coefficient. The experiment was carried out using a setup shown in Fig. 1.

The setup enables a simultaneous precise measurement of the approach and ultrasonic reflectivity as a function of the contact pressure. The contact is realized between the flat rough surface of the upper specimen and the lower specimen: a special head with a smooth surface ($R_a = 0.06\,\mu m$). The quasi-static load is applied gradually (with a 2 MPa step, that provided the rate of loading 1.5 MPa/s), with a special device placed axially in a hydraulic press until a nominal pressure of 800 MPa is reached. The load is measured using a tensometric bridge and the resulting approach of the upper specimen is registered by a displacement (inductive) sensor. The results, in the form of diagrams of the approach versus the contact pressure, are produced on-line on a PC screen. The transmitted ultrasonic signals are reflected and received by a flaw detector (defectoscope, Panametrics-NDT™ EPOCH 4, advanced digital ultrasonic flaw detector; signal processing features include a 25 MHz bandwidth) and passed to a PC for further signal processing, including spectral (frequency) analysis by means of the Fourier transform. The arrangement of the setup ensures a uniform pressure distribution in the contact zone using a precise autoreadjustment of the tested specimen surface against the surface of a gauge head. The contact surface of the head (counterspecimen) is composed of three uniformly placed ring sectors (punches), with the dimensions of approximately $8 \times 8\,mm^2$ each, giving a total contact area of 195 mm² measured during the experiment. Such an arrangement increases the accuracy by the simultaneous measurement on each of the three sectors during one loading of the sample. The counterspecimen has two functions: a loading head and an ultrasonic sender-receiver probe for acoustic waves both in the transverse (T) and normal or longitudinal (L) directions. Three similar piezoelectric transducers are used, with different central frequencies of 4 MHz and 7 MHz for the shear and longitudinal directions, respectively, to predict almost the same wavelengths in steel $\lambda = 0.8\,mm$. The same wavelength for the longitudinal and transverse waves has been chosen to ensure the same conditions of wave interaction with surface imperfections; thus, to create the conditions required in using the "spring model," [14] allowing us to calculate the contact stiffness. We had to obtain wave beams whose axes approximately hit the centers of each punch and cross-section area smaller than the punch cross-section area. A beam width limit is due to the fact that phenomena relating to deformations of the surface layer near the edges of a rough punch pressed in the specimen material differ from those taking place in its flat center. We have decided to use square transducers with 4.5 mm sides for transverse waves and 4.8 mm transducers for longitudinal waves. To ensure the same amplitude of pulses transmitted and received by ultrasonic heads, we have used ceramic parts from the same piezoelectric transducer (PP9 ceramic component, silver electrodes). We have provided for the possibly high repeatability of the process of gluing
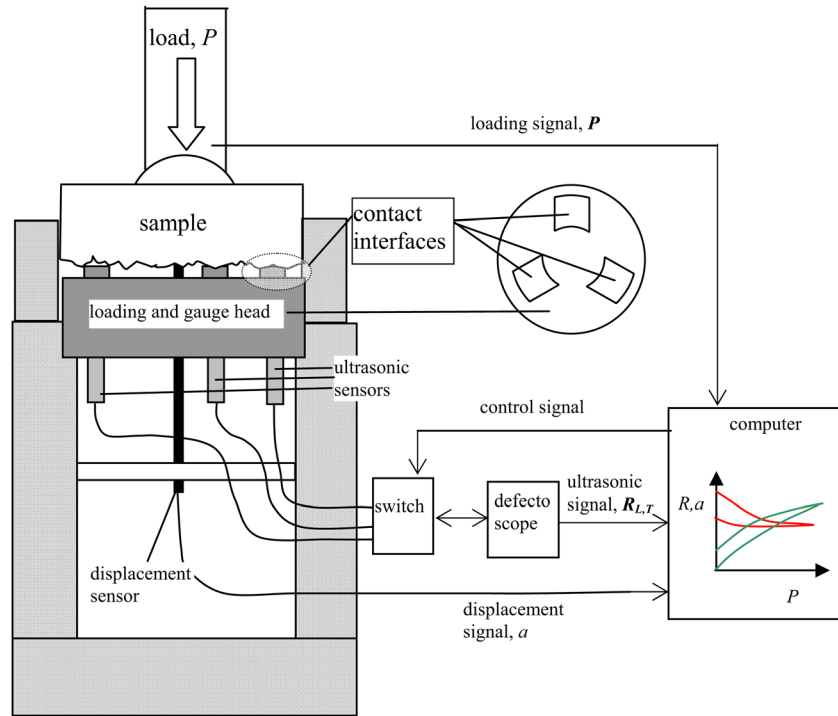
Fig. 1 Schematic experimental setup for the simultaneous measurement of separation *a* and reflection of ultrasonic waves (R_T, R_L) as a function of load *P*

transducers to the punch (preparation of the punch and transducer surfaces, degreasing the surfaces, the same conditions of glue polymerization, and the same pressure of the transducers on the punch). The connection of the transducer with the punch material has to ensure electrical conductivity.

The signal amplitude is measured by a single-channel digital flaw detector by successive switching of the signal input/output to subsequent transmitters. Before loading commences, we measure the specimen amplitude of the original signal R_{ini} (reference) for which the reflection coefficient is maximum and equal to unity. When the specimen load increases, the amplitude of the reflected signal decreases as more and more of the energy passes through the contacting surfaces. The reflection calculated as the ratio of the current amplitude of the reflected signal R to a reference signal R_{ini} decreases to the theoretical value (zero for the contact of two bodies of equal acoustic impedance) for the perfect contact of the two surfaces. In practice, it is not possible to achieve a perfect contact in the case of steel, even with a load much higher than the yield limit and the reflection reaches a minimum value of approximately 0.05. After reaching the preset maximum load, the specimen will unload and the reflection, as a function of the decreasing pressure, is measured. The ultrasonic signal is measured at specific load steps (in our case: 2 MPa). The recorded reflected amplitude signal is converted by a fast Fourier transform to a signal frequency distribution. (First, the same procedure is used for a reference signal, the signal reflected from an unloaded surface). A frequency closest to the resonance frequency of the transducer is selected from the reflected signal spectrum. For that frequency, reflection coefficients are calculated as a ratio of the reflected to the reference signal amplitude for subsequent specimen loads. The values of the reflection coefficients calculated using the spectral analysis of the impulse are well defined for specified frequencies of waves and are not burdened with errors (as is the case with measurements based on comparing the amplitude of the normal pulse) resulting from ultrasonic impulse shape changes occurring during the loading contact. Besides, an ordinary measurement of the maximum signal amplitude is burdened with a larger error because the signal is composed of many frequencies and their

presence in the total reflected signal varies as the specimen is being loaded, leading to a wider scatter of the results.

The setup, simultaneously measuring two quantities is operated by a dedicated control and data collecting program. These quantities are the ultrasonic longitudinal or transverse wave reflection coefficient and an approach of specimens as a function of applied pressure. The principal functions of the program include:

- automatic monitoring of the press load and converting its value to nominal contact stress under the punch surfaces
- reading out values of specimen displacement caused by applied pressure
- control of a multiplexer switching over ultrasonic signals to transducers placed on the respective punches of the counter specimen
- two-way communication with an ultrasonic defectoscope Panametrics Epoch 4, enabling remote setting of its working parameters and recording the results of the pulse measurements
- module of the pulse frequency spectrum analysis, for a fast Fourier transform of recorded pulses and the determination of the frequency characteristics of the reflection coefficient
- presentation of the research results as diagrams of the displacement and reflection coefficient as a function of the contact stress displayed on a computer screen in real time
- recording of the research results for further analysis and presentation by another computer program

Particle displacements in the longitudinal wave propagating in steel are parallel to the direction of wave propagation. This wave, falling perpendicularly to the counterspecimen and samples, is sensitive to the normal stiffness. However, the transverse wave, in which particles carry the vibration perpendicular to the direction of the wave propagation, is sensitive to the tangential stiffness; that is, the ability to transfer shear stresses through the border bodies in contact.

Table 1 Experimental parameters

	Tangential	Longitudinal	
Mass density, ρ	7.7		10^3 kg/m^3
Wave velocity, v	3.1	5.9	10^3 kg/m^3
Wave frequency f, $\omega = 2\pi f$	4	7	10^6 1/s

Table 2 Surface roughness values

Surface roughness parameters			Fine sand blasted	Coarse sand blasted	EDM
Arithmetic mean deviation,	μm	S_a	0.832	5.13	8.94
RMS deviation,	μm	S_q	1.08	6.67	11.62
Maximum height of summits,	μm	S_p	6.1	29.2	48
Maximum depth of valleys,	μm	S_v	4.9	28.8	34
Total height of surface,	μm	S_t	11	58.1	82
Skewness		S_{sk}	0.2	−0.4	0.2
Kurtosis		S_{ku}	3.79	5.08	3.25
Density of summits,	1/mm^2	D_s	573	371	131
Arithmetic mean summits radius,	μm	R	16	6	6

The idea of the measurement is simple. When asperity contact occurs, the ultrasonic waves are transmitted across the interface and where an air gap exists between asperities (parts of the surfaces are not in contact), waves are reflected back and the measured reflection coefficient is almost unity at all wave frequencies. It has been demonstrated by others [19] that the reflection coefficient R_{12} at a partially contacting solid-solid interface is related to the contact stiffness per unit area of the interface, that is expressed by the following formula (if the two materials on either side of the interface are identical)

$$R_{12} = \frac{1}{\sqrt{1 + \left(\dfrac{2K}{\omega z}\right)^2}} \qquad (1)$$

The K quantity present in Eq. (1) is the contact stiffness. Measurement of the K value by mechanical methods is very difficult, especially for a relatively smooth surface, because the approach is often less than 1 μm. Hence, ultrasonic reflection measurements seem to be a good method to determine the value. Rearranging Eq. (1) with a given acoustic impedance $z = \rho v$ and wave frequency (see Table 1), we can calculate the contact stiffness from the reflection measurements as a function of the contact load (see Eq. (1))

$$K = \frac{\omega z}{2}\sqrt{\frac{1}{R_{12}^2} - 1} \qquad (2)$$

The indispensable values used to calculate the normal and tangential stiffness are given in Table 1.

Drinkwater et al. [14] demonstrated that the stiffness of a range of contacts of varying roughness is well represented by Eq. (1). They studied the reflection as a function of the frequency of the ultrasonic wave. The reflection coefficient was found to be dependent on frequency, but the predicted stiffness was shown to be independent of frequency.

3 Results of the Ultrasonic Experiment

The samples for the ultrasonic test were made of carbon steel S45 (0.45% carbon) cylinders, each 50 mm in diameter and 30 mm in height. The surfaces of the contact samples were subjected to three kinds of mechanical treatment: fine and coarse
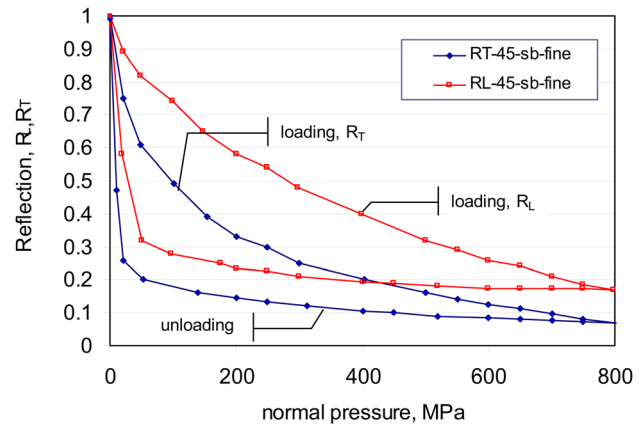
Fig. 2 Tangential R_T and longitudinal R_L reflection coefficient versus loading and unloading (fine sandblasted, $S_a = 0.832\,\mu m$)
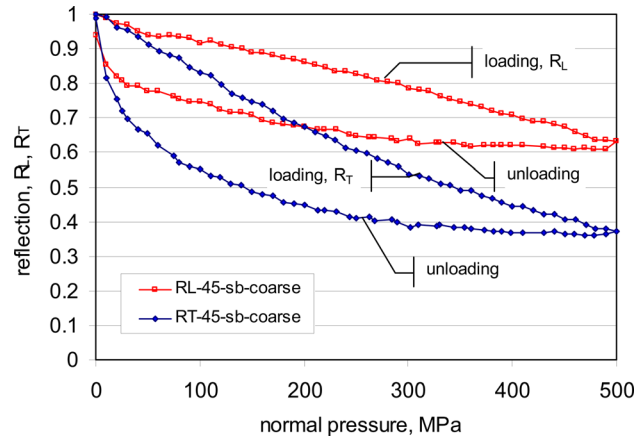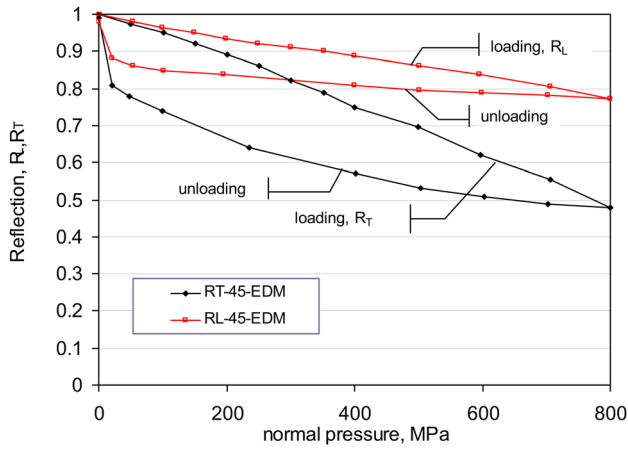

Fig. 3 Tangential R_T and longitudinal R_L reflection coefficient versus loading and unloading (coarse sandblasted, $S_a = 5.13\,\mu m$)
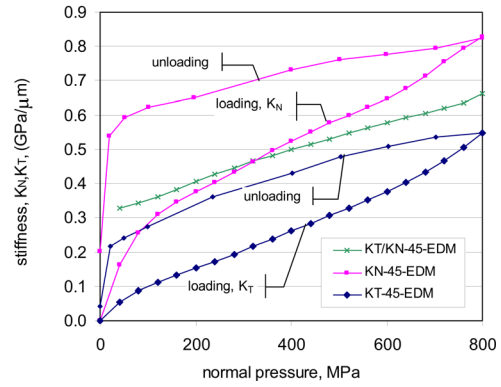
sandblasting and electrical discharge machining. Electrical discharge machining (EDM) is not a typical surface finish method, but it was chosen to yield a very tough isotropic surface of high roughness. The values of profilometric parameters of the examined surfaces are given in Table 2.

The following six diagrams present the results of the ultrasonic wave reflections directly obtained from the device (see Figs. 2–4) and the contact stiffness results (see Figs. 5–7) calculated by formula (2). In all cases the results are shown as a function of the normal load applied and consist of two branches—loading and unloading. The difference in the course of the two branches forms a hysteresis loop for reflectivity and stiffness. The hysteresis is related to the plastic deformation of the asperities and a slower rate of loss of contact during unloading.

The tests led to a number of observations and conclusions. The reflection coefficients decrease monotonically as a function of the increasing load of the contact area, which is related with an increasing real contact area. The values of both reflection coefficients R_L and R_T decrease as a function of the load, with the fastest change occurring for the least rough surface (fine sandblasted), while the slowest change is observed for the roughest surface (electrical discharge machined (EDM)). For the same load value, the transverse wave reflection coefficient is always lower than the longitudinal wave reflection coefficient. For all surfaces, the drops (change rates) of the transverse wave reflection coefficients as a function of the load are significantly larger than the drops of the longitudinal wave reflection coefficients. This means that at the
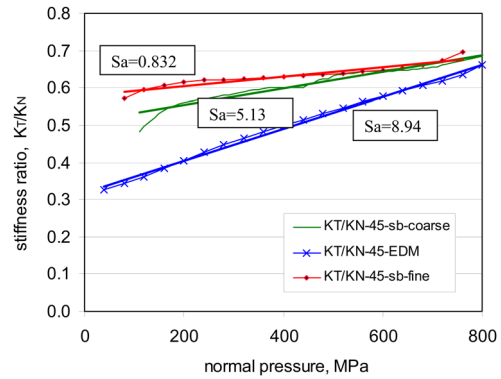
Fig. 4 Tangential R_T and longitudinal R_L reflection coefficient versus loading and unloading (electrical discharge machining (EDM), $S_a = 8.94\,\mu m$)
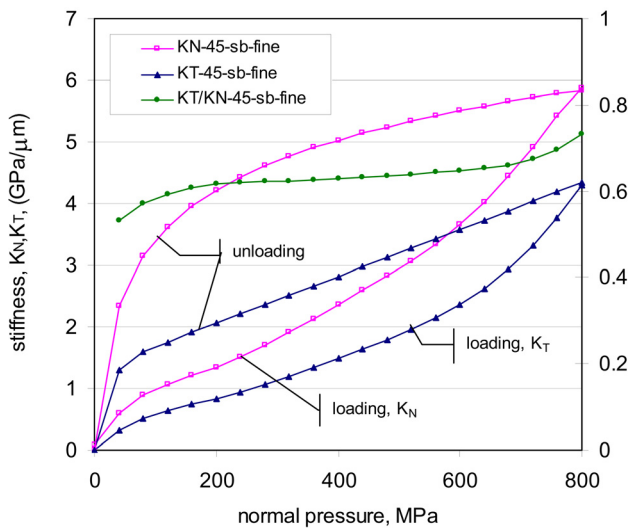
Fig. 5 Tangential K_T and normal K_N contact stiffness and stiffness ratio K_T/K_N (the right-hand scale in the figure) versus loading and unloading (fine sand- blasted, $S_a = 0.832\,\mu m$)

Fig. 6 Tangential K_T and normal K_N contact stiffness and stiffness ratio K_T/K_N versus loading and unloading (coarse sandblasted, $S_a = 5.13\,\mu m$)
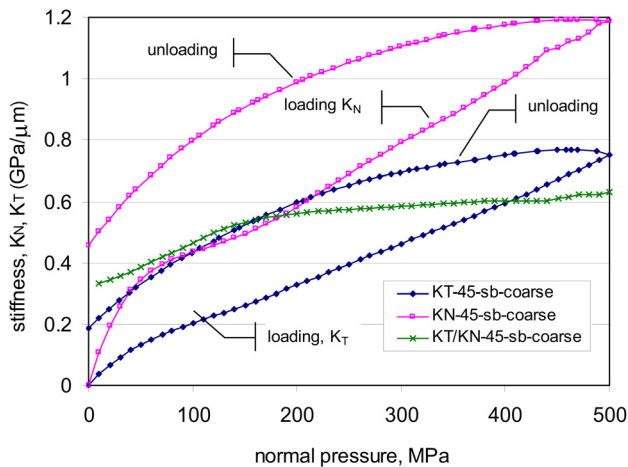

Fig. 7 Tangential K_T and normal K_N contact stiffness and stiffness ratio K_T/K_N versus loading and unloading (electrical discharge machining (EDM), $S_a = 8.94\,\mu m$)

**Fig. 8 Contact stiffness ratio K_T/K_N and linear trends versus loading for all surfaces**

same load of contact surface area and the same wavelength, transverse waves better penetrate the contact surface.

At high loads (exceeding the yield limits of the specimen material) a visible hysteresis occurs; that is, a difference in the dependence of the reflection coefficient during loading and unloading of the contact surface. As predicted, the hysteresis is the smallest for the electrical discharge machined specimen, which is substantially strengthened during surface machining.

During unloading, the value of the longitudinal wave reflection coefficient changes very slowly. Independently of the surface profile (up to 100 MPa) the value of the longitudinal wave reflection coefficient is very small (about only 0.1) and it visibly increases after complete unloading. Slightly higher changes of the reflection coefficient during unloading are observed for the transverse wave. This means that during unloading the real contact area substantially changes after the load is removed.

The contact stiffness grows and reached a maximum, which is about $6\,\mathrm{GPa}/\mu m$ for the least- rough sandblasted surface. As already mentioned for the roughest surface (electrical discharge machined) the contact stiffness is the smallest because it is significantly strengthened. For this reason, it cannot be deformed by flattening roughness peaks when loading increases and, consequently, the contact surface area does not increase. In an intermediate case of the coarse sand-blasted specimen, although relatively rough, the contact stiffness substantially increases. This results from plastic deformation of the roughness peaks, leading to increased contact area.

The relations between the contact stiffness of individual specimens and roughness are in inverse proportion: the higher the roughness, the lower the stiffness. The differences are large: the normal contact stiffness (calculated from the results of L wave
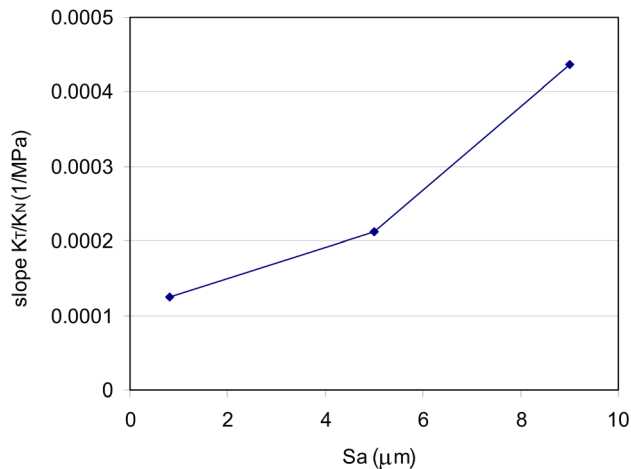
Fig. 9 The slopes of the K_T/K_N trends from Fig. 8 as a function of the roughness amplitude S_a

tests) and tangential stiffness (T wave tests) for a fine sand-blasted surface loaded up to 800 MPa is seven times higher than the stiffness of an EDM surface.

Figure 8 shows a comparison of the tangential to normal contact stiffness ratio K_T/K_N for the examined specimens. All of the measurement results tend to rise slightly as the load increases, with the smallest growth demonstrated by the fine sand-blasted surfaces, and the largest for the EDM surfaces having the greatest roughness. The theoretical assessment of the stiffness ratio presented in Ref. [19] indicates that the K_T/K_N ratio is constant as a function of the load, but for various models it ranges from 0.29 [20] through 0.65 [19,21] to 0.82 [22–24]. This discrepancy most probably results from the assumptions concerning the geometry of the models (the normal distribution of peak heights, spherical shape of asperities, and, in some models, a constant peak radius). Experimental results presented in the literature generally differ much from most theoretical studies in terms of the value and line shape of the K_T/K_N ratio. In the case of our measurements, except for the initial phase of loading to 100 MPa, this relationship is nearly linear (see Fig. 8 (trends)). As the roughness amplitude of the examined surface decreases, the slopes of the trend line gets closer to zero, as in the theoretical models (see Fig. 9).

4 Conclusions

The idea of using ultrasound waves for assessing rough surface contact is not new and we are aware that relevant experiments have been conducted in many places throughout the world. However, there is no standardized well-defined measurement method (e.g., the results in Królikowski and Szczepek [23] are substantially different from ours, while the results in Ref. [19] are similar, even if measured by completely different instruments).

This work presents a unique setup for the simultaneous measurement of the approach and ultrasonic wave reflection coefficient as a function of the rough surface load. The results of the ultrasound measurements have allowed us to calculate the relationship of the contact stiffness as a function of contact loading and unloading. The results of the measurements and calculations are presented for three types of specimens with significantly different roughnesses of $S_a = 0.83 \mu m$, $5.13 \mu m$, and $8.94 \mu m$, respectively. The ten-fold change in the mean roughness amplitude S_a has led to an eight-fold change in the surface stiffness. The experimentally measured ratio of the contact transverse stiffness to the normal stiffness is not constant. Two areas can be distinguished;

for small loads the ratio is strongly nonlinear, while above 100 MPa the K_T/K_N plot is very close to linear. The change of roughness greatly changes the slope representing the ratio. The lower the roughness, the closer to a constant the ratio becomes; thus, closer to theoretical results. The measurement data obtained in this research concerning the contact stiffness have been used for the verification of the authors' theoretical findings based on a fractal description of rough surfaces [25].

References

[1] Ciavarella, M., Murolo, G., Demelio, G., and Barber, J. R., 2004, "Elastic Contact Stiffness and Contact Resistance for the Weierstrass Profile," J. Mech Phys. Solids, **52**, pp. 1247–1265.
[2] Campañá C., Persson, B. N. J., and Müser, M. H., 2011, "Transverse and Normal Interfacial Stiffness With Randomly Rough Surfaces," J. Phys.: Condens. Matter., **23**, p. 085001.
[3] Akarapu, S., Sharp, T., and Robbins, M. O., 2011, "Stiffness of Contact Between Rough Surfaces," Phys. Rev. Lett., **106**, p. 204301.
[4] Medina, S., Nowell, D., and Dini, D., 2013, "Analytical and Numerical Models for Tangential Stiffness of Rough Elastic Contacts," Tribol. Lett., **49**, pp. 103–115.
[5] Pohrt, R. and Popov, V. L., 2012, "Normal Contact Stiffness of Elastic Solids With Fractal Rough Surfaces," Phys. Rev. Lett., **108**, p. 104301.
[6] Pohrt, R., Popov, V. L., and Filipov, A. E., 2012, "Normal Contact Stiffness of Elastic Solids With Fractal Rough Surfaces for One-and Three-Dimensional Systems," Phys. Rev. E, **86**, p. 026710.
[7] Pastewka, L., Prodanov, N., Lorenz, B., Müser, M. H., Robbins, M. O., and Persson, B. N. J., 2013, "Finite-Size Scaling in the Interfacial Stiffness of Rough Elastic Contacts," Phys. Rev. E, **87**, p. 062809.
[8] Campañá C., Müser, M. H., and Robbins, M. O., 2008, "Elastic Contact Between Self-Affine Surfaces: Comparison of Numerical Stress and Contact Correlation Functions With Analytical Predictions," J. Phys.: Condens. Matter, **20**, p. 354013.
[9] Paggi, M. and Barber, J. R., 2011, "Contact Conductance of Rough Surfaces Composed of Modified RMD Patches," Int. J. Heat Mass Transfer, **54**, pp. 4664–4672.
[10] Barber, J. R., 2003, "Bounds on the Electrical Resistance Between Contacting Elastic Rough Bodies," Proc. R. Soc. London, Ser. A, **459**, pp. 53–66.
[11] Barber, J. R., 2013, "Incremental Stiffness and Electrical Conductance in the Contact of Rough Finite Bodies," Phys. Rev. E, **87**, p. 013203.
[12] Kartal, M. E., Mulvihill, D. M., Nowell, D., and Hills, D. A., 2011, "Measurements of Pressure and Area Dependent Tangential Contact Stiffness Between Rough Surfaces Using Digital Image Correlation," Tribol. Int., **44**, pp. 1188–1198.
[13] Quinn, A. M., Dwyer-Joyce, R. S., and Drinkwater, B. W., 2002, "The Measurement of Contact Pressure in Machine Elements Using Ultrasound," Ultrasonics, **39**, pp. 495–502.
[14] Dwyer-Joyce, R. S., Drinkwater, B. W., and Quinn, A. M., 2001, "The Use of Ultrasound in the Investigation of Rough Surface Interfaces," ASME J. Tribol., **123**(1), pp. 8–17.
[15] Lewis, R., Marsha, M. B., and Dwyer-Joyce, R. S., 2005, "Measurement of Interface Pressure in Interference Fit," Proc. Inst. Mech. Eng., Part C, **219**(2), pp. 127–139.
[16] Biwa, S., Hiraiwa, S., and Matsumoto, E., 2007, "Stiffness Evaluation of Contacting Surfaces by Bulk and Interface Waves," Ultrasonics, **46**, pp. 123–129.
[17] Biwa, S., Suzuki, S., and Ohno, N., 2005, "Evaluation of Interface Wave Velocity, Reflection Coefficients and Interfacial Stiffness of Contacting Surfaces," Ultrasonics, **43**, pp. 495–502.
[18] Kim, J. Y., Baltazar, A., and Rokhlin, S. I., 2004, "Ultrasonic Assessment of Rough Surface Contact Between Solids for Elastoplastic Loading-Unloading Hysteresis Cycle," J. Mech. Phys. Solids, **52**, pp. 1911–1934.
[19] Gonzalez-Valadez, M., Baltazar, A., and Dwyer-Joyce, R. S., 2010, "Study of Interfacial Stiffness Ratio of a Rough Surface in Contact Using a Spring Model," Wear, **268**, pp. 373–379.
[20] Yoshioka, N. and Scholtz, C. H., 1989, "Elastic Properties of Contacting Surfaces Under Normal and Shear Loads: Part 1—Theory," J. Geophys. Res., **94**, pp. 17681–17690.
[21] Sherif, H. A. and Kossa, S. S., 1991, "Relationship Between Normal and Tangential Contact Stiffness of Nominally Flat Surfaces," Wear, **151**, pp. 49–62.
[22] Nagy, P. B., 1992, "Ultrasonic Classification of Imperfect Interfaces," J. Nondestruct. Eval., **11**, pp. 127–139.
[23] Królikowski, J. and Szczepek, J., 1993, "Assessment of Tangential and Normal Stiffness of Contact Between Rough Surfaces Using Ultrasonic Method," Wear, **160**, pp. 253–258.
[24] Mindlin, R. D., 1949, "Compliance of Elastic Bodies in Contact," ASME J. Appl. Mech., **71**, pp. 259–268.
[25] Buczkowski, R., Kleiber, M., and Starzynski, G., "Fractal Normal Contact Stiffness of Rough Surfaces," Arch. Mech. (submitted).